Constitutive Activity and Ligand Selectivity of Human, Guinea Pig, Rat, and Canine Histamine H_2 Receptors

Hendrik Preuss, Prasanta Ghorai,[1] Anja Kraus, Stefan Dove, Armin Buschauer, and Roland Seifert

Department of Pharmaceutical/Medicinal Chemistry II, Institute of Pharmacy, University of Regensburg, Regensburg, Germany (H.P., P.G., A.K., S.D., A.B.); and Department of Pharmacology and Toxicology, Institute of Pharmacy, University of Regensburg, Regensburg, Germany (R.S.)

Received January 16, 2007; accepted February 28, 2007

ABSTRACT

Previous studies revealed pharmacological differences between human and guinea pig histamine H_2 receptors (H_2Rs) with respect to the interaction with guanidine-type agonists. Because H_2R species variants are structurally very similar, comparative studies are suited to relate different properties of H_2R species isoforms to few molecular determinants. Therefore, we systematically compared H_2Rs of human (h), guinea pig (gp), rat (r), and canine (c). Fusion proteins of hH_2R, gpH_2R, rH_2R, and cH_2R, respectively, and the short splice variant of $G_{s\alpha}$, $G_{s\alpha S}$, were expressed in Sf9 insect cells. In the membrane steady-state GTPase activity assay, cH_2R-$G_{s\alpha S}$ but neither gpH_2R-$G_{s\alpha S}$ nor rH_2R-$G_{s\alpha S}$ showed the hallmarks of increased constitutive activity compared with hH_2R-$G_{s\alpha S}$, i.e., increased efficacies of partial agonists, increased potencies of agonists with the extent of potency increase being correlated with the corresponding efficacies at hH_2R-$G_{s\alpha S}$, increased inverse agonist efficacies, and decreased potencies of antagonists. Furthermore, in membranes expressing nonfused H_2Rs without or together with mammalian $G_{s\alpha S}$ or H_2R-$G_{s\alpha}$ fusion proteins, the highest basal and GTP-dependent increases in adenylyl cyclase activity were observed for cH_2R. An example of ligand selectivity is given by metiamide, acting as an inverse agonist at hH_2R-$G_{s\alpha S}$, gpH_2R-$G_{s\alpha S}$, and rH_2R-$G_{s\alpha S}$ in the GTPase assay in contrast to being a weak partial agonist with decreased potency at cH_2R-$G_{s\alpha S}$. In conclusion, the cH_2R exhibits increased constitutive activity compared with hH_2R, gpH_2R, and rH_2R, and there is evidence for ligand-specific conformations in H_2R species isoforms.

The histamine H_2 receptor (H_2R) species isoforms of canine (Gantz et al., 1991b), human (Gantz et al., 1991a), rat (Ruat et al., 1991), and guinea pig (Traiffort et al., 1995) were cloned. The four H_2R species isoforms are closely related to each other, as is reflected by an overall amino acid sequence identity of more than 80%. The highest conservation exists within the seven α-helical transmembrane (TM) domains

(sequence identity of more than 90%), whereas the N-terminal domain together with the extracellular end of TM1 and the C terminus are the least conserved regions (Fig. 1).

Despite this high degree of structural similarity, N-[3-(1H-imidazol-4-yl)propyl]guanidines such as compounds **8** to **10** (Fig. 2) differentially activate guinea pig (gpH_2R) and human (hH_2R) H_2 receptors. In a membrane steady-state GTPase activity assay using fusion proteins of H_2R and the short splice variant of $G_{s\alpha}$, $G_{s\alpha S}$, such H_2R-selective agonists are considerably more potent and efficacious at gpH_2R-$G_{s\alpha S}$ than at hH_2R-$G_{s\alpha S}$ (Kelley et al., 2001). By contrast, the small H_2R agonists histamine (**1**, HA), dimaprit (**2**, DIM), amthamine (**3**, AMT), and betahistine (**4**, BET) are unselective between these species. Recently, a novel class of N^G-acylated imida-

ABBREVIATIONS: H_2R, histamine H_2 receptor; TM, transmembrane domain of a G protein-coupled receptor; H_1R, histamine H_1 receptor; gpH_2R, guinea pig histamine H_2 receptor; gpH_2R-$G_{s\alpha S}$, fusion protein of the guinea pig histamine H_2 receptor and the short splice variant of $G_{s\alpha}$; hH_2R, human histamine H_2 receptor; hH_2R-$G_{s\alpha S}$, fusion protein of the human histamine H_2 receptor and the short splice variant of $G_{s\alpha}$; $G_{s\alpha}$, α-subunit of the G_s, protein that mediates adenylyl cyclase activation; $G_{s\alpha S}$, short splice variant of the G_s protein $G_{s\alpha}$; HA, histamine; DIM, dimaprit; AMT, amthamine; BET, betahistine; IMP, impromidine; ARP, arpromidine; CIM, cimetidine; RAN, ranitidine; FAM, famotidine; APT, aminopotentidine; IAPT, iodoaminopotentidine; AC, adenylyl cyclase; GPCR, G protein-coupled receptor; rH_2R, rat histamine H_2 receptor; rH_2R-$G_{s\alpha S}$, fusion protein of the rat histamine H_2 receptor and the short splice variant of $G_{s\alpha}$; S, signal peptide from influenza hemagglutinin; F, FLAG epitope; bp, base pair(s); PAGE, polyacrylamide gel electrophoresis; cH_2R, canine histamine H_2 receptor; cH_2R-$G_{s\alpha S}$, fusion protein of the canine histamine H_2 receptor and the short splice variant of $G_{s\alpha}$; AR, adrenoceptor; ANOVA, analysis of variance.

```
          N-term                TM1                   i1             TM2                  e1
hH2R  MAPNGTASSFCLDSTACKITITVVLAVLILITVAGNVVVCLAVGLNRRLRNLTNCFIVSLAITDLLLGLLVLPFSAIYQLSCKWSFGKVF  90
gpH2R ..F...VP...M.F.VY.V..S.I.II...V.......................S...........V...........................S...  90
rH2R  .E....VH.C...M.L.V..S...TT.....I.............S......S........A..........................FT...H...  90
cH2R  .IS...G.......PP.R..VS...T......I.............S...........................F.....R......  90

          TM3                   i2                    TM4               e2
hH2R  CNIYTSLDVMLCTASILNLFMISLDRYCAVMDPLRYPVLVTPVRVAISLVLIWVISITLSFLSIHLGWNSRNETSKGNHTTSKCKVQVNE  180
gpH2R .........................................T........I.A......F................D.D.IV.  180
rH2R  .........................................T........F..............G.RG..D.F-........  179
cH2R  .........................................T......I....V.....................SF...IP.......L  180

          TM5              i3                        TM6               e3
hH2R  VYGLVDGLVTFYLPLLIMCITYYRIFKVARDQAKRINHISSWKAATIREHKATVTLAAVMGAFIICWFPYFTAFVYRGLRGDDAINEVLE  270
gpH2R ..................F....I..E..R.....G..................V......K....V...F.  270
rH2R  ...............V....I..E................................AV.  269
cH2R  .............V....I....H.MG......G..............V......K......AF.  270

          TM7                        C-term
hH2R  AIVLWLGYANSALNPILYAALNRDFRTGYQQLFCCRLANRNSHKTSLRSNASQLSRTQSREPRQQEEKPLKLQVWSGTEVTAPQGATDR  359
gpH2R DV..............A.H.........SH...E....L.N...N.S.CQ...W..D...N.................N.  359
rH2R  G...............A......H.KF.SH.........L.N.L.P.S.....G.W...............L.H...NPI.  358
cH2R  .V...............T......A.....R..P.SH.AQE......S...A.N.....MR.................R....  359
```

Fig. 1. Comparison of the amino acid sequences of hH2R, gpH2R, rH2R, and cH2R. The amino acid sequences of hH2R, gpH2R, rH2R, and cH2R are given in the one-letter code. Dots in the sequences of gpH2R, rH2R, and cH2R indicate identity with hH2R. Amino acids shown in white with black shading represent the interaction sites of HA with the H2R (Gantz et al., 1992; Nederkoorn et al., 1996). The most conserved residues (X.50 with X being the number of the TM domain, according to the Ballesteros/Weinstein nomenclature) in each TM domain are indicated in gray shading. Amino acids shown in regular font in the sequences of gpH2R, rH2R, and cH2R represent conservative exchanges. Amino acids shown in bold in the sequences of gpH2R, rH2R, and cH2R represent nonconservative exchanges. N-term, extracellular N-terminal domain of H2Rs; C-term, intracellular C-terminal domain of H2Rs; i1, i2, and i3, first, second, and third intracellular loops; e1, e2, e3, first, second, and third extracellular loops, respectively.

zolylpropylguanidines as represented by compounds **11** to **16** was developed (Ghorai, 2005; Xie et al., 2006a). Generally, by introduction of a carbonyl group adjacent to the guanidine moiety, the species selectivity of the agonists is preserved (Xie et al., 2006a). Comparison of the corresponding agonist efficacies in the GTPase assay and at stabilizing the high-affinity ternary complex of the H2R with nucleotide-free $G_{s\alpha}$ indicate that N-[3-(1H-imidazol-4-yl)propyl]guanidines and their N^G-acylated analogs stabilize different ligand-specific active conformations of hH2R and gpH2R (Kelley et al., 2001; Xie et al., 2006a). However, it is not known whether these differences also apply for other H2R species isoforms. Moreover, H2Rs are known to be constitutively active (Alewijnse et al., 1998), but the degree to which constitutive activity varies among several species isoforms remains elusive. To generate an expanded pharmacological profile of H2R species isoforms, in the present report, we compare human, guinea pig, rat, and canine H2Rs.

Sf9 cell membranes expressing H2R-$G_{s\alpha S}$ fusion proteins were used to measure steady-state GTPase activity. For this purpose, we studied several classes of H2R ligands (Fig. 2). HA (**1**) and related small H2R agonists DIM (**2**), AMT (**3**), and BET (**4**) similarly interact with the binding site of H2R. The amino group of HA forms an ionic interaction with Asp-98(3.32) in TM3, and the imidazolyl ring presumably interacts with Tyr-182(5.38) and Asp-186(5.42) in TM5 (Fig. 1). The guanidine-type H2R agonists impromidine (**8**, IMP), arpromidine (**9**, ARP), and BU-E-43 (**10**), as well as the N^G-acylated derivatives **11** to **16** share a common N-[3-(1H-imidazol-4-yl)propyl)]guanidine moiety that mimics binding of HA and thus is crucial for agonistic activity (Dove et al.,

2004). The 2-(5-methylimidazol-4-ylmethylthio)ethyl moiety of IMP and the 3-(4-fluorophenyl)-3-(2-pyridyl)propyl group of ARP are supposed to interact with a pocket formed by multiple residues in TM3, -6, and -7 (Kelley et al., 2001). The variable side chains of the ARP derivatives **10** to **16** consist of diverse mono- or diarylalkyl groups with different chain lengths between the aromatic ring system and the guanidine group. In compound **16** (Xie et al., 2006b), the aryl ring is replaced by a cyclohexyl moiety. Compound **13** is the pure (R)-enantiomer (eutomer). 2-Benzylhistamine (**5**) and supra-histaprodifen (**6**) represent H1R agonists with partial H2R agonism (Seifert et al., 2003). Burimamide (**7**) and metiamide (**22**) are neutral H2R antagonists, whereas cimetidine (**17**, CIM), ranitidine (**18**, RAN), famotidine (**19**, FAM), aminopotentidine (**20**, APT), and iodoaminopotentidine (**21**, IAPT) act as inverse agonists (Hill et al., 1997; Dove et al., 2004).

Previous studies showed that the determination of adenylyl cyclase (AC) activity in Sf9 cell membranes is a very sensitive system to elucidate differences in the constitutive activities of GPCRs (Seifert et al., 1998b). Therefore, we also assessed AC activity in membranes expressing nonfused H2Rs (coupling to endogenous $G_{s\alpha}$-like G proteins), in membranes coexpressing H2R and mammalian $G_{s\alpha S}$, and in membranes expressing H2R-$G_{s\alpha S}$ fusion proteins.

Materials and Methods

Materials. The cDNA for the rH2R was kindly provided by Dr. R. Leurs (Leiden/Amsterdam Center for Drug Research, Department of Medicinal Chemistry, Vrije Universiteit Amsterdam, Amsterdam, The Netherlands) (Ruat et al., 1991). The cDNA for the cH2R was
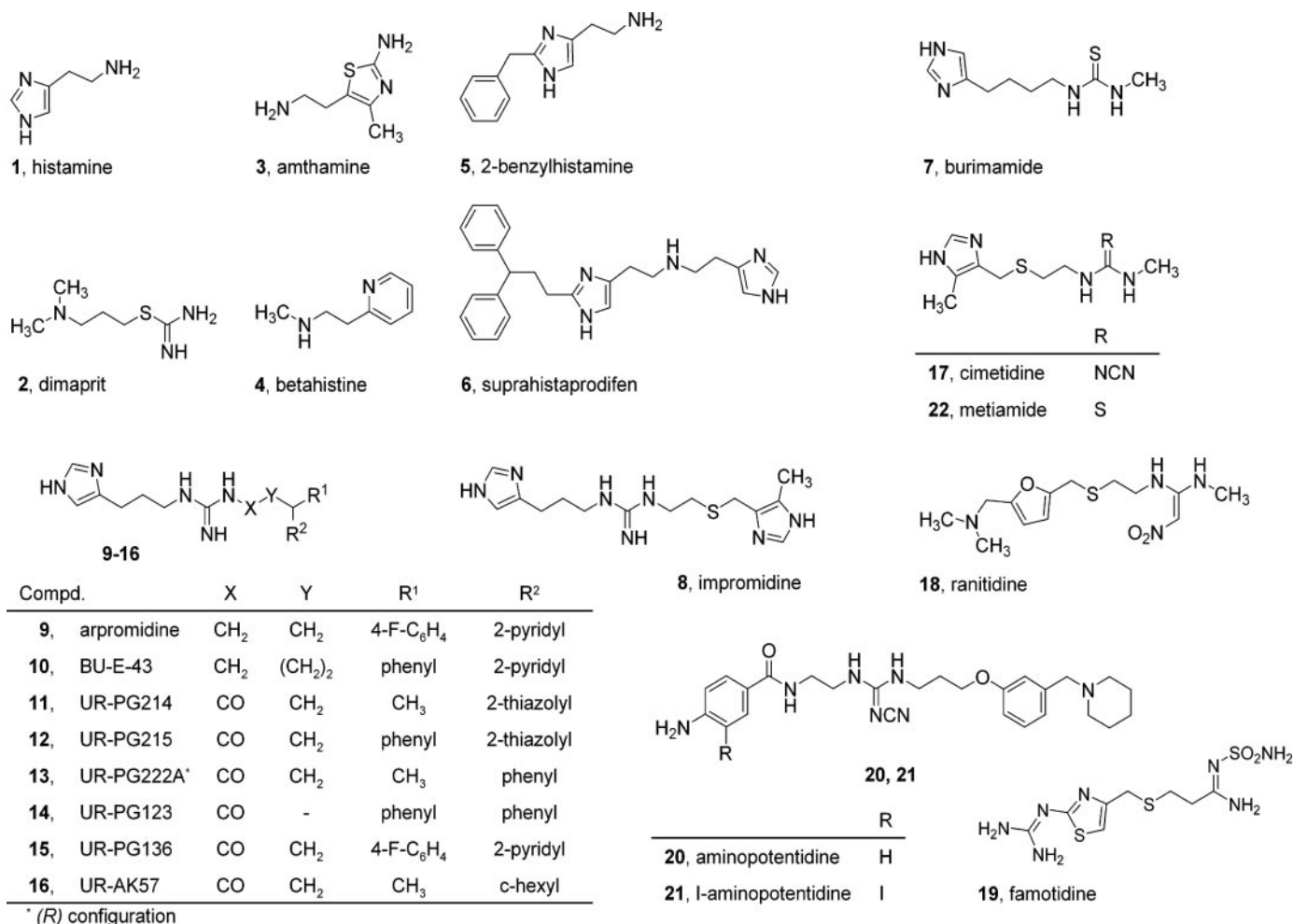
Fig. 2. Structures of H₂R agonists, partial agonists, and antagonists. 1 to 4, small H₂R agonists; 5 and 6, H₁R agonists with partial agonism at the H₂R; 8 to 10, guanidine-type H₂R agonists; 11 to 16, N^G-acylated N-[3-(1H-imidazol-4-yl)propyl]guanidines with agonistic H₂R activity; 7 and 17 to 22, H₂R antagonists.

kindly provided by Dr. I. Gantz (University of Michigan, Medical School and Ann Arbor VA Medical Center, Ann Arbor, MI) (Gantz et al., 1991b). The generation of the baculoviruses encoding hH₂R, gpH₂R, hH₂R-G$_{s\alpha S}$, and gpH₂R-G$_{s\alpha S}$ was described previously (Kelley et al., 2001; Houston et al., 2002). The baculoviruses encoding G$_{s\alpha S}$ were kindly provided by Drs. R. Sunahara and A. G. Gilman (Department of Pharmacology, University of Southwestern Medical Center, Dallas, TX). The generation of pGEM-3Z-SF-β_1AR-G$_{s\alpha S}$ and pVL1392-SF-β_1AR-G$_{s\alpha S}$ was described previously (Wenzel-Seifert et al., 2002). Compounds **11** through **15** (Ghorai, 2005; Xie et al., 2006a) and compound **16** (Xie et al., 2006b) were prepared as described previously (Ghorai, 2005). The preparation of IMP, ARP, BU-E-43, APT, and IAPT was described previously (Dove et al., 2004). Suprahistaprodifen and 2-benzylhistamine were synthesized as described previously (Elz et al., 2000; Seifert et al., 2003). The structures of compounds were confirmed by analysis (C, H, N), ¹H NMR, and mass spectrometry. Purity of compounds was >98% as determined by high-performance liquid chromatography or capillary electrophoresis. The anti-FLAG Ig (M1 monoclonal antibody) was from Sigma-Aldrich (St. Louis, MO). The anti-G$_s\alpha$ Ig (C-terminal) was from Santa Cruz Biotechnology (Santa Cruz, CA), and the anti-His₆ Ig was from Clonetech (Mountain View, CA). [γ-³²P]GTP (6000 Ci/mmol), [α-³²P]ATP (800 Ci/mmol), and [³H]dihydroalprenolol (85–90 Ci/mmol) were from PerkinElmer Life and Analytical Sciences (Boston, MA). All unlabeled nucleotides were from Roche Diagnostics (Indianapolis, IN). HA, BET, CIM, RAN, and FAM were from Sigma-Aldrich. AMT was from Tocris Cookson Inc. (Ballwin, MO). DIM was

from Sigma/RBI (Natick, MA). Burimamide and metiamide were from Dr. W. Schunack (Free University of Berlin, Berlin, Germany). All restriction enzymes, T4 DNA ligase, and calf intestinal phosphatase were from New England Biolabs (Beverly, MA). Cloned *Pfu* DNA polymerase was from Stratagene (La Jolla, CA).

Construction of the cDNAs for rH₂R and rH₂R-G$_{s\alpha S}$. The cDNAs encoding for the proteins were generated by sequential overlap-extension PCRs. With pGEM-3Z-SF-gpH₂R-G$_{s\alpha S}$ as template, PCR 1A was used to amplify a DNA fragment consisting of the cleavable signal peptide from influenza hemagglutinin (S), the FLAG epitope (F) recognized by the M1 monoclonal antibody, and the start codon of the rH₂R. The sense primer annealed with 18 bp of pGEM-3Z before the 5′ end of SF. The antisense primer annealed with 15 bp of the 3′ end of SF and with ATG. In PCR 1B, the cDNA encoding the rH₂R followed by a hexahistidine tag in 3′ position was generated. The hexahistidine tag was included to allow future purification and to provide additional protection against proteolysis (Seifert et al., 1998a). The sense primer consisted of 15 bp of the 3′ end of SF and the first 22 bp of the 5′ end of the rH₂R. The antisense primer consisted of 18 bp of the C terminus of the rH₂R, the hexahistidine tag, the stop codon, and an XbaI site. The cDNA for the rH₂R was extracted from pcDNA-rH₂R after restriction digestion with HindIII and BglII and was used as template. In PCR 2, the products of PCR 1A and PCR 1B annealed in the region encoding SF and ATG. Here, the sense primer of PCR 1A and the antisense primer of PCR 1B were used. In that way, a fragment encoding SF, the rH₂R, the hexahistidine tag, the stop codon, and an XbaI site was

obtained. This fragment was digested with SacI and XbaI and cloned into pGEM-3Z-SF-hH$_2$R digested with SacI and XbaI to yield pGEM-3Z-SF-rH$_2$R. pGEM-3Z-SF-rH$_2$R was digested with SacI and XbaI and cloned into the baculovirus transfer vector pVL1392-SF-hH$_2$R digested with SacI and XbaI. With pGEM-3Z-SF-rH$_2$R as template, the sense primer of PCR 1A, and an antisense primer encoding six histidines, in PCR 3A a fragment encoding SF, the cDNA for the rH$_2$R, and the hexahistidine tag was generated. In PCR 3B, a fragment encoding the hexahistidine tag, the cDNA of G$_{s\alpha S}$, the stop codon, and an XbaI site was generated. Here, the sense primer annealed with the hexahistidine tag and the start codon of G$_{s\alpha S}$, and the antisense primer annealed with the cDNA encoding the five C-terminal amino acids of G$_{s\alpha S}$, the stop codon, and an XbaI site. pGEM-3Z-SF-gpH$_2$R-G$_{s\alpha S}$ was used as template. In PCR 4, the products of PCRs 3A and 3B annealed in the hexahistidine region, and the sense primer of PCR 1A and the antisense primer of PCR 3B were used. In that way, the complete cDNA for the rH$_2$R-G$_{s\alpha S}$ fusion protein, consisting of SF, the cDNA for the rH$_2$R, the hexahistidine tag, and the cDNA of G$_{s\alpha S}$ was amplified. The product of PCR 4 was digested with SacI and BglII and cloned into pGEM-3Z-SF-β_1AR-G$_{s\alpha S}$ digested with SacI and BglII. In addition, the PCR 4 product was digested with SacI and BglII and directly cloned into pVL1392-SF-β_1AR-$_{Gs\alpha S}$ that was digested with SacI and BglII and treated with calf intestinal phosphatase to yield the baculovirus transfer vector pVL1392-SF-rH$_2$R-G$_{s\alpha S}$.

Construction of the cDNAs for cH$_2$R and cH$_2$R-G$_{s\alpha S}$. The strategy for the generation of the cDNAs for the epitope-tagged cH$_2$R and cH$_2$R-G$_{s\alpha S}$ was analogous to the strategy for the generation of the cDNAs for rH$_2$R and rH$_2$R-G$_{s\alpha S}$. With pGEM-3Z-SF-gpH$_2$R-G$_{s\alpha S}$ as template, in PCR 1A the SF region and the start codon of the cH$_2$R were amplified. The sense primer annealed with 18 bp of pGEM-3Z before the 5′ end of SF, and the antisense primer annealed with 15 bp of the 3′ end of SF and with ATG. In PCR 1B, the cDNA encoding the sequence for the cH$_2$R followed by the hexahistidine tag in 3′ position was generated. The sense primer consisted of 15 bp of the 3′ end of SF and the first 21 bp of the 5′ end of cH$_2$R. The antisense primer consisted of 18 bp of the C terminus of the cH$_2$R, the hexahistidine tag, the stop codon, and an XbaI site. The cDNA for the cH$_2$R was extracted from CMVneo-cH$_2$R after digestion with BglII and was used as template. In PCR 2, the products of PCR 1A and PCR 1B annealed in the region encoding SF and ATG. Here, the sense primer of PCR 1A and the antisense primer of PCR 1B were used. In that way, a fragment encoding SF, the cH$_2$R, the hexahistidine tag, the stop codon, and an XbaI site was obtained. This fragment was digested with SacI and XbaI and cloned into pGEM-3Z-SF-hH$_2$R digested with SacI and XbaI to yield pGEM-3Z-SF-cH$_2$R. pGEM-3Z-SF-cH$_2$R was digested with SacI and XbaI and cloned into the baculovirus transfer vector pVL1392-SF-hH$_2$R digested with SacI and XbaI. PCR 3 was used to generate a fragment encoding the C terminus of the cH$_2$R, the hexahistidine tag, and G$_{s\alpha S}$. The sense primer encoded the last 10 amino acids of the C terminus of the cH$_2$R, the hexahistidine tag, and the start codon of G$_{s\alpha S}$, and the antisense primer encoded the five C-terminal amino acids of G$_{s\alpha S}$, the stop codon, and an XbaI site. Here, pGEM-3Z-SF-hH$_2$R-G$_{s\alpha S}$ was used as template. This fragment was digested with XhoI and XbaI and cloned into pGEM-3Z-SF-cH$_2$R digested with XhoI and XbaI to yield pGEM-3Z-SF-cH$_2$R-G$_{s\alpha S}$. pGEM-3Z-SF-cH$_2$R-GsαS was digested with SacI and BglII and cloned into pVL1392-SF-β_1AR-G$_{s\alpha S}$ that was digested with SacI and BglII and treated with calf intestinal phosphatase to yield the baculovirus transfer vector pVL1392-SF-cH$_2$R-G$_{s\alpha S}$.

Generation of Recombinant Baculoviruses, Cell Culture, and Membrane Preparation. Recombinant baculoviruses encoding rH$_2$R, cH$_2$R, rH$_2$R-G$_{s\alpha S}$, and cH$_2$R-G$_{s\alpha S}$ were generated in Sf9 cells using the BaculoGOLD transfection kit (BD Biosciences PharMingen, San Diego, CA) according to the manufacturer's instructions. After initial transfection, high-titer virus stocks were generated by two sequential virus amplifications. Sf9 cells were cultured in 250-ml

disposable Erlenmeyer flasks at 28°C under rotation at 125 rpm in SF 900 II medium (Invitrogen, Carlsbad, CA) supplemented with 5% (v/v) fetal calf serum (Cambrex Bio Science Walkersville Inc., Walkersville, MD) and 0.1 mg/ml gentamicin (Cambrex Bio Science Walkersville Inc.). Cells were maintained at a density of 0.5 to 6.0 × 10^6 cells/ml. For infection, cells were sedimented by centrifugation and suspended in fresh medium. Cells were seeded at 3.0 × 10^6 cells/ml and infected with a 1:100 dilution of high-titer baculovirus stocks encoding H$_2$Rs, G$_{s\alpha S}$, and H$_2$R-G$_{s\alpha S}$ fusion proteins. Cells were cultured for 48 h before membrane preparation. Sf9 membranes were prepared as described previously (Seifert et al., 1998a), using 1 mM EDTA, 0.2 mM phenylmethylsulfonyl fluoride, 10 μg/ml benzamidine, and 10 μg/ml leupeptin as protease inhibitors. Membranes were suspended in binding buffer (12.5 mM MgCl$_2$, 1 mM EDTA, and 75 mM Tris-HCl, pH 7.4) and stored at −80°C until use.

SDS-PAGE and Immunoblot Analysis. Membrane proteins were separated on SDS polyacrylamide gels containing 12% (w/v) acrylamide. Proteins were then transferred onto Immobilon-P transfer membranes (Millipore Corporation, Bedford, MA). Membranes were reacted with M1 antibody, anti-G$_{s\alpha}$ Ig, or anti-His$_6$ Ig (1:1000 each). Immunoreactive bands were visualized by enhanced chemoluminescence (Pierce Chemical, Rockford, IL) using sheep anti-mouse IgG (M1 and anti-His$_6$ Ig) and donkey anti-rabbit IgG (anti-G$_{s\alpha}$ Ig), respectively, coupled to peroxidase.

Steady-State GTPase Activity Assay. Membranes were thawed, sedimented, and resuspended in 10 mM Tris-HCl, pH 7.4. Assay tubes contained Sf9 membranes expressing H$_2$R-G$_{s\alpha S}$ fusion proteins (10 μg of protein/tube), 1.0 mM MgCl$_2$, 0.1 mM EDTA, 0.1 mM ATP, 100 nM GTP, 0.1 mM adenylyl imidodiphosphate, 5 mM creatine phosphate, 40 μg of creatine kinase, and 0.2% (w/v) bovine serum albumin in 50 mM Tris-HCl, pH 7.4, and H$_2$R ligands at various concentrations. Reaction mixtures (80 μl) were incubated for 2 min at 25°C before the addition of 20 μl of [γ-^{32}P]GTP (0.1 μCi/tube). All stock and work dilutions of [γ-^{32}P]GTP were prepared in 20 mM Tris-HCl, pH 7.4. Reactions were conducted for 20 min at 25°C. Preliminary studies under basal conditions and with HA, IMP, and ARP showed that under these conditions, GTP hydrolysis was linear. Reactions were terminated by the addition of 900 μl of slurry consisting of 5% (w/v) activated charcoal and 50 mM NaH$_2$PO$_4$, pH 2.0. Charcoal absorbs nucleotides but not P$_i$. Charcoal-quenched reaction mixtures were centrifuged for 7 min at room temperature at 15,000g. Six hundred microliters of the supernatant fluid of reaction mixtures was removed, and ^{32}P$_i$ was determined by liquid scintillation counting. Enzyme activities were corrected for spontaneous degradation of [γ-^{32}P]GTP. Spontaneous [γ-^{32}P]GTP degradation was determined in tubes containing all of the above-described components plus a very high concentration of unlabeled GTP (1 mM) that, by competition with [γ-^{32}P]GTP, prevents [γ-^{32}P]GTP hydrolysis by enzymatic activities present in Sf9 membranes. Spontaneous [γ-^{32}P]GTP degradation was <1% of the total amount of radioactivity added using 20 mM Tris-HCl, pH 7.4, as solvent for [γ-^{32}P]GTP. The experimental conditions chosen ensured that not more than 10% of the total amount of [γ-^{32}P]GTP added was converted to ^{32}P$_i$.

AC Activity Assay. AC activity in Sf9 membranes was determined as described previously (Houston et al., 2002). In brief, membranes were thawed and sedimented by a 15-min centrifugation at 4°C and 15,000g to remove residual endogenous guanine nucleotides as far as possible, and they were subsequently resuspended in binding buffer. Tubes contained Sf9 membranes expressing H$_2$Rs (100 μg of protein/tube), H$_2$Rs coexpressed with mammalian G$_{s\alpha S}$ (50 μg of protein/tube), or H$_2$R-G$_{s\alpha S}$ fusion proteins (20 μg of protein/tube), additionally 5 mM MgCl$_2$, 0.4 mM EDTA, and 30 mM Tris-HCl, pH 7.4. Assay tubes containing membranes and various additions in a total volume of 30 μl were incubated for 3 min at 37°C before starting reactions by the addition of 20 μl of reaction mixture containing (final) [α-^{32}P]ATP (0.3 μCi/tube) plus 40 μM unlabeled ATP, 2.7 mM mono(cyclohexyl)ammonium phosphoenolpyruvate, 0.125 IU of pyruvate kinase, 1 IU of myokinase, and 0.1 mM cAMP. Reactions were

conducted for 20 min at 37°C. Reactions were terminated by the addition of 20 μl of 2.2 N HCl. Denatured protein was sedimented by a 3-min centrifugation at 25°C and 15,000g. Sixty-five microliters of the supernatant fluid was applied onto disposable columns filled with 1.3 g of neutral alumina (Sigma A-1522, super I, WN-6). [^{32}P]cAMP was separated from [α-^{32}P]ATP by elution of [^{32}P]cAMP with 4 ml of 0.1 M ammonium acetate, pH 7.0. Recovery of [^{32}P]cAMP was ~80%. Blank values were routinely ~0.01% of the total amount of [α-^{32}P]ATP added. [^{32}P]cAMP was determined by liquid scintillation counting. The experimental conditions chosen ensured that not more than 1 to 3% of the total amount of [α-^{32}P]ATP added was converted to [^{32}P]cAMP.

Miscellaneous. Protein concentrations were determined using the DC protein assay kit (Bio-Rad, Hercules, CA). [^{3}H]Dihydroalprenolol saturation binding was performed as described previously (Seifert et al., 1998a). All analyses of experimental data were performed with the Prism 4 program (GraphPad Software Inc., San Diego, CA). K_B values were calculated using the Cheng and Prusoff equation (1973) equation. Expression levels of recombinant proteins were determined using the Bio-Rad GS-710 calibrated imaging densitometer and the software tool Quantity One, version 4.0.3 (Bio-Rad).

Results

Immunological Detection of Recombinant Proteins in Sf9 Cell Membranes. The predicted molecular mass of the H$_2$R is ~33 kDa (Gantz et al., 1991a,b; Fukushima et al., 1997). H$_2$R species isoforms presumably exhibit similar glycosylation patterns, because the putative N-glycosylation sites for the H$_2$R, Asn-4, and Asn-162 are fully conserved within their sequences (Fig. 1) (Fukushima et al., 1995). However, only rH$_2$R and hH$_2$R migrated as the expected bands for monomeric GPCRs (Fig. 3, A and B). Both bands occur as doublets, representing different glycosylation forms (Houston et al., 2002). Additional bands were detected at ~70

kDa, presumably representing receptor dimers. A similar pattern of immunoreactive bands was previously observed for the hH$_2$R (Houston et al., 2002). In contrast, both cH$_2$R and gpH$_2$R displayed strong doublet bands at ~60 kDa that coincide with the expected bands of differentially glycosylated H$_2$R dimers, whereas the bands for monomers were absent. Additional bands were detected at ~150 kDa and above 250 kDa, possibly corresponding to H$_2$R tetramers and higher oligomers, respectively. Dimerization and oligomerization of the cH$_2$R has been described previously (Fukushima et al., 1997), but in those experiments, also receptor monomers were detected. Hence, gpH$_2$R and cH$_2$R possibly migrated atypically in SDS-PAGE, i.e., the bands at ~60 and ~150 kDa could correspond to monomers and dimers, respectively, and not to dimers and tetramers. With the anti-His$_6$ Ig, in membranes expressing cH$_2$R, an additional doublet band at ~23 kDa was detected, and in rH$_2$R- and hH$_2$R membranes, an ~27-kDa band was present. However, no such bands were detected in gpH$_2$R membranes. The ~23–27-kDa bands may represent differentially and atypically migrating H$_2$R monomers not recognized by the M1 antibody because of a lack of epitope exposure. By analogy to formyl peptide receptors (Wenzel-Seifert and Seifert, 2003) differences in the C termini of H$_2$R species isoforms may constitute the molecular basis for the species-selective migration pattern. Thus, H$_2$R species isoforms are well expressed in Sf9 membranes, but due to their widely different migration, it is impossible to precisely assess their expression levels using β_2AR-membranes calibrated with [^{3}H]dihydroalprenolol saturation binding as standard (Kelley et al., 2001).

H$_2$R-G$_{s\alpha S}$ fusion proteins of canine, rat, guinea pig, and human occurred as strong bands at ~80 kDa (Fig. 3C). Because G$_{s\alpha S}$ has an apparent molecular mass of ~45 kDa, these bands correspond to H$_2$R-G$_{s\alpha S}$ monomers. Weaker
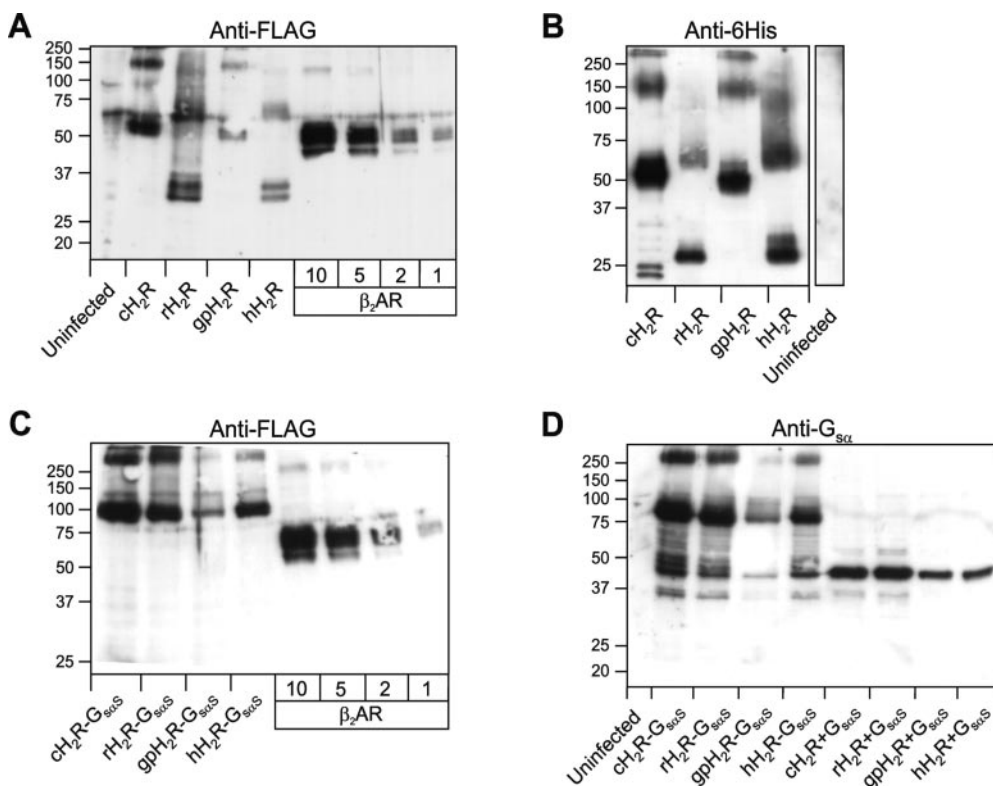
Fig. 3. Immunological detection and analysis of the expression of recombinant proteins in Sf9 cells. Sf9 membranes expressing various proteins were prepared, separated by SDS-PAGE on gels containing 12% (w/v) acrylamide, transferred onto Immobilon-P membranes, and probed with the respective Ig indicated on top of each panel. In each lane, 10 μg of membrane protein was loaded onto the gel, unless otherwise indicated below membranes. Exceptionally, 40 μg of a membrane expressing gpH$_2$R-G$_{s\alpha S}$ were loaded onto the gels in C and D. Numbers on the left of membranes designate masses of marker proteins in kilodaltons. In A and C, 1, 2, 5, and 10 μg of protein of Sf9 membranes expressing the β_2AR at 7.5 pmol mg^{-1} (as determined by [^{3}H]DHA saturation binding) were used as standard to assess the expression levels of H$_2$R species isoforms. In D, membranes expressing H$_2$R-G$_{s\alpha S}$ fusion proteins and membranes coexpressing H$_2$R species and mammalian G$_{s\alpha S}$ were loaded onto the gel.

bands were detected at ~110 kDa, most probably representing differently glycosylated fusion proteins. With all species, additional bands at ~250 kDa were detected, presumably representing H_2R-$G_{s\alpha S}$ dimers or oligomers. cH_2R-$G_{s\alpha S}$ was expressed at ~5 pmol mg^{-1}, rH_2R-$G_{s\alpha S}$ at ~4 pmol mg^{-1}, gpH_2R-$G_{s\alpha S}$ at ~1 pmol mg^{-1}, and hH_2R-$G_{s\alpha S}$ at ~3 pmol mg^{-1} using β_2AR-membranes as standard. To account for the decreased expression level of gpH_2R-$G_{s\alpha S}$, in this case the amount of protein applied to the gel was adjusted to 40 μg.

Probing membranes expressing H_2R-$G_{s\alpha S}$ species with the anti-$G_{s\alpha}$ Ig yielded ~80- and ~250-kDa bands (Fig. 3D), which are consistent with those bands observed with the anti-FLAG Ig. Additional bands occurred at ~45 kDa, representing atypically migrating or partially degraded fusion proteins. In all membranes coexpressing H_2R species and $G_{s\alpha S}$, the expected bands for $G_{s\alpha S}$ monomers were detected at ~45 kDa. The expression levels of $G_{s\alpha S}$ in membranes coexpressing H_2R and $G_{s\alpha S}$ were estimated using the ~80-kDa peak intensities of H_2R-$G_{s\alpha S}$ species as standard and were ~2 pmol mg^{-1} in membranes coexpressing cH_2R and $G_{s\alpha S}$, ~2 pmol mg^{-1} in membranes coexpressing rH_2R and $G_{s\alpha S}$, ~1 pmol mg^{-1} in membranes coexpressing gpH_2R and $G_{s\alpha S}$, and ~1 pmol mg^{-1} in membranes coexpressing hH_2R and $G_{s\alpha S}$.

Efficacies and Potencies of Agonists at H_2R-$G_{s\alpha S}$ Species Isoforms Derived from the GTPase Assay. Efficacies and potencies of compounds **1** to **22** at H_2R-$G_{s\alpha S}$ fusion proteins of human, guinea pig, rat, and canine are summarized in Table 1. The small H_2R agonists acted as full (**1-3**) or as nearly full (**4**) agonists at the four receptors with approximately similar efficacies. HA (**1**) and DIM (**2**) were equipotent at human, guinea pig, and rat H_2R-$G_{s\alpha S}$, they but showed lower EC_{50} values at cH_2R-$G_{s\alpha S}$. AMT (**3**) was slightly more potent at cH_2R-$G_{s\alpha S}$ than at hH_2R-$G_{s\alpha S}$ and gpH_2R-$G_{s\alpha S}$. At rH_2R-$G_{s\alpha S}$, the potency of AMT (**3**) was further decreased. BET (**4**) acted with increased potencies at gpH_2R-$G_{s\alpha S}$ and cH_2R-$G_{s\alpha S}$, compared with hH_2R-$G_{s\alpha S}$ and rH_2R-$G_{s\alpha S}$. In agreement with previous studies (Kelley et al., 2001; Xie et al., 2006a,b), N-[3-(1H-imidazol-4-yl)propyl]guanidines (**8-10**) and their N^G-acylated analogs (**11-16**) were more potent and more efficacious at gpH_2R-$G_{s\alpha S}$ than at hH_2R-$G_{s\alpha S}$ (Table 1). At gpH_2R-$G_{s\alpha S}$, UR-PG222A (**13**) was more efficacious than HA (**1**). At hH_2R-$G_{s\alpha S}$ and rH_2R-$G_{s\alpha S}$, the compounds exhibited similar efficacies and potencies. Only UR-PG214 (**11**) was slightly more potent at rH_2R-$G_{s\alpha S}$ than at hH_2R-$G_{s\alpha S}$. Apart from ARP (**9**) and its N^G-acylated analog UR-PG136 (**15**) that acted with similar efficacies at cH_2R-$G_{s\alpha S}$ and hH_2R-$G_{s\alpha S}$, compounds **8** to **16** were more efficacious at cH_2R-$G_{s\alpha S}$ than at hH_2R-$G_{s\alpha S}$. Compounds **8** to **16** were also more potent at cH_2R-$G_{s\alpha S}$ than at hH_2R-$G_{s\alpha S}$. An exception of this rule was UR-PG123 (**14**) that exhibited the largest efficacy increase (~4-fold) but was somewhat less potent at cH_2R-$G_{s\alpha S}$ than at hH_2R-$G_{s\alpha S}$. In summary, small H_2R agonists **1** to **4** acted with similar efficacies at all H_2R-$G_{s\alpha S}$ species isoforms investigated, but they were more potent at cH_2R-$G_{s\alpha S}$ compared with hH_2R-$G_{s\alpha S}$, gpH_2R-$G_{s\alpha S}$, and rH_2R-$G_{s\alpha S}$. Guanidines and N^G-acylated guanidines **8** to **16** acted with increased efficacies and potencies at gpH_2R-$G_{s\alpha S}$ and cH_2R-$G_{s\alpha S}$ compared with hH_2R-$G_{s\alpha S}$, whereas no selectivity was observed between rH_2R-$G_{s\alpha S}$ and hH_2R-$G_{s\alpha S}$.

Compounds **5** and **6** are representatives of H_1R agonists with partial H_2R agonism (Seifert et al., 2003). Both compounds were less efficacious at gpH_2R-$G_{s\alpha S}$ than at hH_2R-

$G_{s\alpha S}$ and similarly efficacious at rH_2R-$G_{s\alpha S}$ and hH_2R-$G_{s\alpha S}$ (Table 1). In the GTPase assay at H_2R-$G_{s\alpha S}$ fusion proteins, burimamide (**7**) was a weak partial agonist with similar efficacies at human, guinea pig, and rat species. Strikingly, compounds **5**, **6**, and **7** acted with significantly increased efficacies at cH_2R-$G_{s\alpha S}$ compared with hH_2R-$G_{s\alpha S}$. Apart from 2-benzylhistamine (**5**) with ~2-fold increased potency at gpH_2R-$G_{s\alpha S}$, the potencies of **5** to **7** did not significantly differ between the species investigated. Taken together, partial H_2R agonists were considerably more efficacious at cH_2R-$G_{s\alpha S}$ than at human, guinea pig, and rat H_2R-$G_{s\alpha S}$.

Potencies and Inverse Agonist Efficacies of Antagonists at H_2R-$G_{s\alpha S}$ Species Isoforms Derived from the GTPase Assay. K_B values and inverse agonist efficacies of the H_2R antagonists CIM (**17**), RAN (**18**), FAM (**19**), APT (**20**), and IAPT (**21**) are listed in Table 2. The compounds decreased GTPase activities below basal values and thus acted as inverse agonists at all four species. At hH_2R-$G_{s\alpha S}$ and gpH_2R-$G_{s\alpha S}$ compounds **17** to **21** decreased the basal GTPase signal (0%) by ~10% if the maximal stimulatory effect of 100 μM HA was set to 100%. At rH_2R-$G_{s\alpha S}$ the inverse agonist efficacies of **17** to **21** were somewhat smaller. At cH_2R-$G_{s\alpha S}$ all compounds except CIM (**17**) showed a significantly higher reduction of the basal GTPase activity by ~20%. The K_B values of **17** to **21** were similar at hH_2R-$G_{s\alpha S}$ and gpH_2R-$G_{s\alpha S}$. At rH_2R-$G_{s\alpha S}$, **17** to **19** were less potent, and **20** and **21** were similarly potent compared with hH_2R-$G_{s\alpha S}$. By contrast, all compounds except FAM (**19**) were less potent at cH_2R-$G_{s\alpha S}$ than at hH_2R-$G_{s\alpha S}$. Taken together, most of the H_2R antagonists studied displayed increased inverse agonist efficacies and decreased potencies at cH_2R-$G_{s\alpha S}$ compared with hH_2R-$G_{s\alpha S}$.

Constitutive Activities of hH_2R-$G_{s\alpha S}$, gpH_2R-$G_{s\alpha S}$, rH_2R-$G_{s\alpha S}$, and cH_2R-$G_{s\alpha S}$ in the GTPase Assay. As was reported for a constitutively activated mutant of the β_2AR (Samama et al., 1993), the following major hallmarks distinguish constitutively active GPCRs from not (quiescent) or less constitutively active GPCRs. First, the efficacies of partial agonists are increased at the more constitutively active receptor. To uncover differences in the constitutive activities among H_2R-$G_{s\alpha S}$ species, efficacies of partial and full agonists **1** to **16** and inverse agonist efficacies of antagonists **17** to **21** were compared at hH_2R-$G_{s\alpha S}$ with gpH_2R-$G_{s\alpha S}$, rH_2R-$G_{s\alpha S}$, and cH_2R-$G_{s\alpha S}$, respectively (Fig. 4, A, C, and E). Second, constitutively active receptors exhibit an increased affinity for agonists but not antagonists, with the extent of affinity increase being correlated with the efficacy of the ligand (Lefkowitz et al., 1993). Essentially, the potencies in the GTPase assay represent apparent affinities and can be therefore related, as $logEC_{50}$ differences between hH_2R-$G_{s\alpha S}$ and the other H_2R species isoforms, to the corresponding efficacies at hH_2R-$G_{s\alpha S}$ (Fig. 4, B, D, and F). Finally, at receptors with increased constitutive activity inverse agonists have an elevated inhibitory effect on GTP hydrolysis (Seifert et al., 1998b).

Similar inverse agonist efficacies of antagonists **17** to **21** and the absence of selectivity in the efficacies of partial agonists **5** to **7** and **14** indicate equal magnitudes of constitutive activities for gpH_2R-$G_{s\alpha S}$ and hH_2R-$G_{s\alpha S}$ (Fig. 4A). As Fig. 4B illustrates, a poor but significant correlation ($r^2 = 0.27$; $p = 0.016$) was observed between the log (potency ratio) of these species and the efficacies of compounds **1** to **21** at

TABLE 1

Agonist efficacies and potencies at H$_2$R-G$_{soS}$ species isoforms in the GTPase assay

Steady-state GTPase activity in Sf9 membranes expressing hH$_2$R-G$_{soS}$, gpH$_2$R-G$_{soS}$, rH$_2$R-G$_{soS}$, and cH$_2$R-G$_{soS}$ was determined as described under *Materials and Methods*. Reaction mixtures contained Sf9 membranes expressing fusion proteins and agonists at concentrations from 1 nM to 1 mM as appropriate to generate saturated concentration-response curves. Curves were analyzed by nonlinear regression and were best fitted to sigmoidal concentration-response curves. Typical basal GTPase activities ranged between ~1 and 2 pmol mg^{-1} min^{-1}, and the maximal stimulatory effect of HA (100 μM) amounted to 400 to 600% above basal. To calculate agonist efficacies, the maximal stimulatory effect of histamine was set at 1.00, and the stimulatory effects of other agonists were referred to this value. Data shown are the means ± S.D. of three to five experiments performed in duplicate. Efficacies and potencies, respectively, of ligands at hH$_2$R-G$_{soS}$ were compared with the corresponding parameters at gpH$_2$R-G$_{soS}$, rH$_2$R-G$_{soS}$ and cH$_2$R-G$_{soS}$, respectively, using one-way ANOVA. The control data for hH$_2$R-G$_{soS}$ and gpH$_2$R-G$_{soS}$ are identical with the control data for these constructs in Table 1 of Preuss et al. (2007).

Compound	hH$_2$R-G$_{soS}$		gpH$_2$R-G$_{soS}$		rH$_2$R-G$_{soS}$		cH$_2$R-G$_{soS}$	
	Efficacy	EC$_{50}$	Efficacy[a]	EC$_{50}$[b]	Efficacy	EC$_{50}$	Efficacy[a]	EC$_{50}$[b]
		nM		nM		nM		nM
1 HA	1.00	990 ± 92	1.00	850 ± 340	1.00	1200 ± 16	1.00	290 ± 50[++]
2 DIM	0.85 ± 0.02	910 ± 430	0.94 ± 0.06*	740 ± 360	0.89 ± 0.03	1100 ± 92	0.90 ± 0.04	480 ± 82
3 AMT	0.91 ± 0.02	190 ± 50	1.04 ± 0.01**	190 ± 42	0.91 ± 0.03	360 ± 100[+]	0.82 ± 0.03**	110 ± 66
4 BET	0.81 ± 0.07	44,000 ± 8900	0.72 ± 0.02	28,000 ± 4400[+]	0.71 ± 0.03	47,000 ± 9100	0.78 ± 0.08	27,000 ± 6900[+]
5 2-Benzylhistamine	0.45 ± 0.05	13,000 ± 1000	0.26 ± 0.01**	6800 ± 1900[++]	0.43 ± 0.01	13,000 ± 1000	0.68 ± 0.02**	13,000 ± 1200
6 Suprahistaprodifen	0.54 ± 0.08	240 ± 41	0.43 ± 0.02*	310 ± 62	0.43 ± 0.02*	400 ± 81[+]	0.77 ± 0.03**	260 ± 18
7 Burimamide	0.16 ± 0.01	14,000 ± 12,000	0.17 ± 0.02	12,000 ± 3600	0.18 ± 0.02	15,000 ± 2100	0.40 ± 0.01**	11,000 ± 210
8 IMP	0.82 ± 0.02	160 ± 42	0.96 ± 0.06	18 ± 9[+]	0.99 ± 0.06*	110 ± 9	0.99 ± 0.10*	41 ± 18[++]
9 ARP	0.84 ± 0.03	72 ± 9	0.94 ± 0.05*	7 ± 1[++]	0.80 ± 0.03	90 ± 7[++]	0.84 ± 0.07	10 ± 1[++]
10 BU-E-43	0.71 ± 0.11	130 ± 13	0.87 ± 0.05	43 ± 10[++]	0.70 ± 0.04	140 ± 22	0.88 ± 0.05*	46 ± 6[++]
11 UR-PG214	0.91 ± 0.08	130 ± 45	0.94 ± 0.05	25 ± 10[++]	1.03 ± 0.06	84 ± 8	1.00 ± 0.06	28 ± 8[++]
12 UR-PG215	0.80 ± 0.04	120 ± 45	0.94 ± 0.05*	14 ± 4[+]	0.82 ± 0.06	96 ± 12	0.99 ± 0.05**	40 ± 10[++]
13 UR-PG222A	0.90 ± 0.04	18 ± 6	1.18 ± 0.08**	5 ± 1[++]	0.93 ± 0.01	13 ± 1	0.98 ± 0.03	3 ± 2[++]
14 UR-PG123	0.14 ± 0.03	250 ± 13	0.40 ± 0.02**	220 ± 22	0.15 ± 0.02	250 ± 48	0.59 ± 0.02**	340 ± 33[+]
15 UR-PG136	0.82 ± 0.05	100 ± 9	1.02 ± 0.11*	29 ± 10[++]	0.73 ± 0.02	100 ± 16	0.86 ± 0.08	52 ± 4[++]
16 UR-AK57	0.86 ± 0.05	15 ± 4	0.97 ± 0.18	14 ± 6	0.73 ± 0.02	14 ± 1	0.92 ± 0.03	5 ± 3[+]
22 Metiamide	−0.08 ± 0.01	1400 ± 900	−0.06 ± 0.01	750 ± 460	−0.04 ± 0.01**	670 ± 510	0.06 ± 0.01**	21,000 ± 2200[++]

[a] Comparison with the efficacy at hH$_2$R-G$_s\alpha_S$; *, $p < 0.05$; **, $p < 0.01$.
[b] Comparison with the EC$_{50}$ value at hH$_2$R-G$_s\alpha_S$; [+], $p < 0.05$; [++], $p < 0.01$.

TABLE 2

Potencies and inverse agonist efficacies of antagonists at H_2R-$G_{s\alpha S}$ species isoforms in the GTPase assay

Steady-state GTPase activity in Sf9 membranes expressing hH_2R-$G_{s\alpha S}$, gpH_2R-$G_{s\alpha S}$, rH_2R-$G_{s\alpha S}$, and cH_2R-$G_{s\alpha S}$ was determined as described under *Materials and Methods*. Reaction mixtures contained Sf9 membranes expressing fusion proteins, 1 μM HA as agonist and antagonists at concentrations from 1 nM to 100 μM as appropriate to generate saturated competition curves. Competition curves were analyzed by nonlinear regression. To determine the inverse agonist efficacies (Inv. Ago. Eff.), the effects of antagonists at fixed concentrations (10 μM of 18–21; 100 μM of 17) on basal GTPase activity were assessed and referred to the stimulatory effect of 100 μM HA (=1.00). Data shown are the means ± S.D. of three experiments performed in duplicates. K_B values and inverse agonist efficacies, respectively, of antagonists at hH_2R-$G_{s\alpha S}$ were compared with the corresponding parameters at gpH_2R-$G_{s\alpha S}$, rH_2R-$G_{s\alpha S}$, and cH_2R-$G_{s\alpha S}$, respectively, using one-way ANOVA. The control data for hH_2R-$G_{s\alpha S}$ and gpH_2R-$G_{s\alpha S}$ are identical with the control data for these constructs in Table 2 of Preuss et al. (2007).

	Compound	hH_2R-$G_{s\alpha S}$		gpH_2R-$G_{s\alpha S}$		rH_2R-$G_{s\alpha S}$		cH_2R-$G_{s\alpha S}$	
		K_B	Inv. Ago. Eff.	K_B[a]	Inv. Ago. Eff.	K_B[a]	Inv. Ago. Eff.[b]	K_B	Inv. Ago. Eff.[b]
		nM		*nM*		*nM*		*nM*	
17	CIM	1700 ± 430	−0.08 ± 0.01	1300 ± 270	−0.09 ± 0.02	2800 ± 340*	−0.06 ± 0.01	7500 ± 400**	−0.07 ± 0.02
18	RAN	840 ± 94	−0.09 ± 0.01	1000 ± 170	−0.08 ± 0.01	2100 ± 410**	−0.06 ± 0.01[++]	1500 ± 160*	−0.18 ± 0.01[++]
19	FAM	48 ± 10	−0.10 ± 0.02	38 ± 3	−0.10 ± 0.01	91 ± 7**	−0.07 ± 0.01[+]	59 ± 1	−0.22 ± 0.01[++]
20	APT	180 ± 12	−0.09 ± 0.01	260 ± 43*	−0.09 ± 0.01	170 ± 27	−0.06 ± 0.01[+]	620 ± 49**	−0.20 ± 0.01[++]
21	IAPT	35 ± 7	−0.10 ± 0.01	26 ± 4	−0.10 ± 0.01	32 ± 8	−0.07 ± 0.01[++]	83 ± 21**	−0.22 ± 0.01[++]

[a] Comparison with the K_B value at hH_2R-$G_{s\alpha S}$; *, $p < 0.05$; **, $p < 0.01$.
[b] Comparison with Inv. Ago. Eff. at hH_2R-$G_{s\alpha S}$; [+], $p < 0.05$; [++], $p < 0.01$.

hH_2R-$G_{s\alpha S}$. However, this correlation was determined by ligand-specific interactions, namely, the high potencies of guanidines (**8** to **10**) and N^G-acylguanidines (**11** to **16**) at gpH_2R-$G_{s\alpha S}$ (Kelley et al., 2001; Xie et al., 2006a,b), and disappeared if only compounds **1** to **7** and **17** to **21** were considered ($r^2 = 0.04$; $p = 0.527$). The efficacies of compounds **1** to **21** at rH_2R-$G_{s\alpha S}$ and hH_2R-$G_{s\alpha S}$ were almost identical (Fig. 4C). Moreover, no correlation between the log (potency ratio) and the efficacies at hH_2R-$G_{s\alpha S}$ was evident ($r^2 = 0.16$; $p = 0.077$) (Fig. 4D). Thus, in the steady-state GTPase assay, rH_2R-$G_{s\alpha S}$ and hH_2R-$G_{s\alpha S}$ exhibited similar levels of constitutive activities. By contrast, cH_2R-$G_{s\alpha S}$ showed the hallmarks of a GPCR with increased constitutive activity compared with hH_2R-$G_{s\alpha S}$. Specifically, partial agonists **5** to **7** and **14** were considerably more efficacious at cH_2R-$G_{s\alpha S}$ and the inverse agonist efficacies of antagonists **18** to **21** were increased compared with hH_2R-$G_{s\alpha S}$ (Fig. 4E). A highly significant correlation between the log (potency ratio) and the efficacies of compounds **1** to **21** at hH_2R-$G_{s\alpha S}$ was determined ($r^2 = 0.77$; $p < 0.0001$; Fig. 4F). It is noteworthy that this correlation was independent of distinct interactions of guanidines and N^G-acylguanidines with cH_2R-$G_{s\alpha S}$ as omitting compounds **8** to **16** did not change the fit ($r^2 = 0.75$; $p = 0.0003$).

Ambiguous Response of Metiamide (22) in the GTPase Assay. At hH_2R-$G_{s\alpha S}$, metiamide (**22**) decreased the basal GTPase signal by 8 ± 1% and thus acted as weak inverse agonist (Table 1; Fig. 5). At gpH_2R-$G_{s\alpha S}$ and rH_2R-$G_{s\alpha S}$, metiamide inhibited the basal GTPase signals by 6 ± 1 and 4 ± 1%, respectively, and was ~2-fold more potent than at hH_2R-$G_{s\alpha S}$. Intriguingly, at cH_2R-$G_{s\alpha S}$ metiamide did not act as an inverse agonist but rather as a very weak partial agonist (efficacy of 6 ± 1%). This is in marked contrast to the results of antagonists **18** to **21** reducing the basal GTPase signal at cH_2R-$G_{s\alpha S}$ (increased constitutive activity) more effectively than at the other less constitutively active species. Furthermore, the potency of **22** was lowered by approximately 15-fold compared with hH_2R-$G_{s\alpha S}$ and not increased as would have been expected for a partial agonist (Samama et al., 1993). Attempts to detect changes in AC activity upon stimulation with metiamide in membranes coexpressing cH_2R and $G_{s\alpha S}$ failed due to the much lower sensitivity of this system compared with the GTPase activity assay using fusion proteins (data not shown).

Regulation of AC Activities in Membranes Expressing Fused and Nonfused H_2R Species Isoforms. AC activity was measured in Sf9 cell membranes expressing H_2Rs (coupling to endogenous $G_{s\alpha}$-like G proteins), in membranes coexpressing H_2R and mammalian $G_{s\alpha S}$, and in membranes expressing H_2R-$G_{s\alpha S}$ fusion proteins. Basal AC activities were similar in membranes expressing hH_2R, gpH_2R, and rH_2R (Table 3) and ~2-fold higher in the case of the cH_2R. GTP (10 μM) by itself increased AC activities at all four H_2R species by ~2-fold above the basal level. HA (**1**) further increased, and IAPT (**21**) inhibited this GTP-dependent signal increase, indicative for constitutive activity of all four H_2R species isoforms in Sf9 membranes (Fig. 6, A–D). These observations are in agreement with previous studies at the β_2AR (Seifert et al., 1998a). The stimulatory effects of GTP, as determined by relating the effects of GTP (10 μM) to the effects of HA (100 μM) plus GTP (10 μM), were largest at cH_2R and rH_2R, compared with hH_2R and gpH_2R. Both the high basal AC activity and the strong stimulation with GTP indicate an elevated level of constitutive activity in membranes expressing the cH_2R relative to membranes expressing hH_2R, gpH_2R, and rH_2R. It is noteworthy that the constitutive activity of rH_2R seemed to be slightly increased compared with hH_2R and gpH_2R.

The GPCR/G protein stoichiometry affects the magnitude of response (Kenakin, 2001). In H_2R membranes coexpressing mammalian $G_{s\alpha S}$, 5- to 18-fold increased basal levels of AC activity were measured relative to membranes expressing H_2R alone (Table 3). Basal AC activities were ~6-fold higher at cH_2R plus $G_{s\alpha S}$ and ~2-fold higher at rH_2R plus $G_{s\alpha S}$, respectively, compared with hH_2R plus $G_{s\alpha S}$. With gpH_2R plus $G_{s\alpha S}$, the basal AC activity was somewhat lower than with hH_2R plus $G_{s\alpha S}$. As was observed in membranes expressing H_2R alone, the highest stimulatory effects of GTP in the coexpression system were observed with cH_2R and rH_2R compared with gpH_2R and hH_2R. The inverse agonist IAPT (10 μM) decreased the GTP-dependent increases of AC activity at all species isoforms (Fig. 6, E–H), but even strongly reduced basal AC activities at the lowest concentrations of added GTP. These effects were probably due to traces of GDP being converted to GTP by the action of nucleoside diphosphate kinase and were most prominent in membranes expressing cH_2R plus $G_{s\alpha S}$ (~69% reduction below basal) and rH_2R plus $G_{s\alpha S}$ (~59% reduction), compared with hH_2R plus
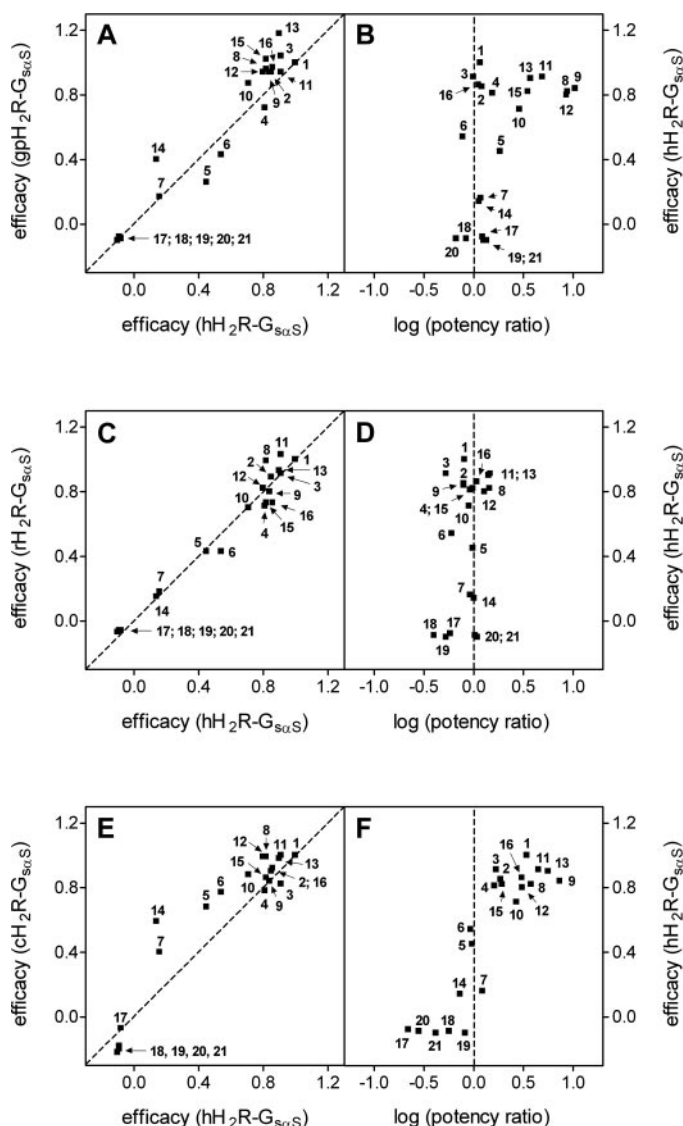
Fig. 4. Efficacies and potencies of ligands 1 to 21 at hH_2R-$G_{s\alpha S}$ in pairwise comparison with gpH_2R-$G_{s\alpha S}$, rH_2R-$G_{s\alpha S}$, and cH_2R-$G_{s\alpha S}$, respectively, as determined in the steady-state GTPase assay. GTPase activity in Sf9 membranes was measured as described under *Materials and Methods*. Data shown are the means taken from Tables 1 and 2. A, C, and E, relation between the efficacies of compounds 1 to 21 at hH_2R-$G_{s\alpha S}$ versus gpH_2R-$G_{s\alpha S}$ (A), rH_2R-$G_{s\alpha S}$ (C), and cH_2R-$G_{s\alpha S}$ (E), respectively. The dashed line has a slope of 1.0 and represents a theoretical curve of identical efficacies in both systems. B, D, and F, relation between log (potency ratio) of compounds 1 to 21 at gpH_2R-$G_{s\alpha S}$ (B), rH_2R-$G_{s\alpha S}$ (D), and cH_2R-$G_{s\alpha S}$ (F), respectively, and the corresponding efficacies at hH_2R-$G_{s\alpha S}$. The potency ratio is the ratio of EC_{50} values of full and partial agonists (1–16) at hH_2R-$G_{s\alpha S}$ and at gpH_2R-$G_{s\alpha S}$, rH_2R-$G_{s\alpha S}$, and cH_2R-$G_{s\alpha S}$, respectively. Accordingly, the potency ratio of antagonists (17–21) is the ratio of the corresponding K_B values at hH_2R-$G_{s\alpha S}$ and at gpH_2R-$G_{s\alpha S}$, rH_2R-$G_{s\alpha S}$, and cH_2R-$G_{s\alpha S}$, respectively. The vertical dashed line intersects the abscissa at 0.0 and represents a theoretical curve of identical potencies in both systems.

$G_{s\alpha S}$ (~29% reduction) and gpH_2R plus $G_{s\alpha S}$ (~23% reduction). Taken together, among H_2R species isoforms coexpressed with $G_{s\alpha S}$, cH_2R was the most constitutively active GPCR.

Due to the efficient coupling of the signaling partners in GPCR-$G_s\alpha$ fusion proteins (Seifert et al., 1999), in membranes expressing H_2R-$G_{s\alpha S}$, strongly elevated basal AC activities were measured, compared with membranes express-
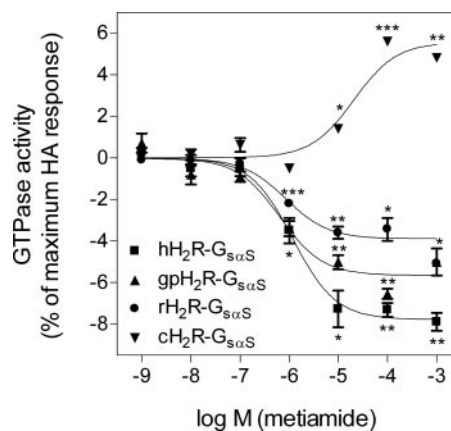
Fig. 5. Effects of metiamide on GTPase activity in membranes expressing H_2R-$G_{s\alpha S}$ species isoforms. GTPase activity in Sf9 membranes was determined as described under *Materials and Methods*. Reaction mixtures contained membranes (10 μg of protein/tube) expressing hH_2R-$G_{s\alpha S}$, gpH_2R-$G_{s\alpha S}$, rH_2R-$G_{s\alpha S}$, and cH_2R-$G_{s\alpha S}$ fusion proteins and metiamide at concentrations indicated on the abscissa. Data are expressed as percentage change in GTPase activity induced by metiamide compared with the GTPase activity stimulated by HA (100 μM). Data shown are the means ± S.E.M. of three independent experiments performed in duplicates. Data were analyzed by nonlinear regression and were best fitted to sigmoidal concentration-response curves. The significance of the deviation from zero was calculated for each mean value using t test; *, $p < 0.05$; **, $p < 0.01$; ***, $p < 0.001$.

ing nonfused H_2Rs coexpressing $G_{s\alpha S}$ (Table 3). In agreement with the results obtained for membranes expressing nonfused H_2Rs, among the four species isoforms, cH_2R-$G_{s\alpha S}$ and rH_2R-$G_{s\alpha S}$ exhibited the highest basal AC activities. As shown in Fig. 6, K and L, GTP increased AC activity in those membranes so effectively that HA could not produce a further increase, reflecting exhaustion of the limiting pool of AC molecules (Seifert at al., 1998a). At hH_2R-$G_{s\alpha S}$ and gpH_2R-$G_{s\alpha S}$, GTP induced only smaller increases, allowing HA to further enhance AC activity. By contrast, in the absence of added GTP, HA (100 μM) yielded a reduction of basal AC activities at all four species (Fig. 6, I–L). Very similar effects were observed previously for the β_2AR-$G_{s\alpha S}$ fusion protein (Seifert et al., 1998b) and are due to dissociation of GDP from $G_{s\alpha S}$ following agonist binding to the receptor without subsequent binding of GTP. Because $G_{s\alpha\text{-}GDP}$ is more effective in activating AC than nucleotide-free $G_{s\alpha}$, AC activity was reduced below basal. Due to much less efficient coupling in membranes coexpressing receptors and $G_{s\alpha S}$ (Seifert et al., 1998a; Houston et al., 2002; Gille and Seifert, 2003), in this case HA did not reduce basal AC activity (Fig. 6, E–H). Similar differences in the coupling efficiencies between fusion proteins and nonfused expression systems were observed in terms of ternary complex formation, guanosine 5′-O-(3-thio)triphosphate binding, GTP hydrolysis, and AC activation in the presence of GTP (Seifert et al., 1998a; Wenzel-Seifert et al., 2002; Gille and Seifert, 2003). Thus, in membranes expressing H_2R-$G_{s\alpha S}$ fusion proteins the apparent constitutive activities were considerably higher than in membranes expressing nonfused H_2Rs. In the case of cH_2R-$G_{s\alpha S}$ and rH_2R-$G_{s\alpha S}$, saturation of AC molecules became manifest upon agonist (HA) stimulation.

Discussion

Increased Constitutive Activity of the cH_2R Compared with hH_2R, gpH_2R, and rH_2R. The use of GPCR-

TABLE 3

AC activities in Sf9 membranes expressing H_2R species isoforms without or with $G_{s\alpha S}$, and in Sf9 membranes expressing H_2R-$G_{s\alpha S}$ fusion proteins

Basal AC activities and the effects of GTP and HA on AC activity were assessed. AC activity in Sf9 membranes was determined as described under *Materials and Methods*. Reaction mixtures contained Sf9 membranes expressing 20 to 100 μg protein/tube as appropriate and distilled water (basal), GTP (10 μM), or GTP (10 μM), and HA (100 μM). Data shown are the means ± S.D. of three to four experiments performed in triplicates. To calculate the stimulatory effect of GTP (Rel. GTP Effect), the effect of GTP (10 μM) was referred to the effect of GTP (10 μM) plus HA (100 μM). The control data for hH_2R-$G_{s\alpha S}$ and gpH_2R-$G_{s\alpha S}$ are identical with the control data for these constructs in Table 3 of Preuss et al. (2007).

	Basal, AC Activity	10 μM GTP, AC Activity	10 μM GTP + 100 μM HA, AC Activity	Rel. GTP Effect
	pmol mg^{-1} min^{-1}			%
hH_2R	0.3 ± 0.0	0.6 ± 0.1	3.4 ± 0.2	10
gpH_2R	0.3 ± 0.1	0.5 ± 0.0	2.6 ± 0.2	9
rH_2R	0.4 ± 0.0	0.8 ± 0.1	3.1 ± 0.2	15
cH_2R	0.7 ± 0.1	1.5 ± 0.2	4.3 ± 0.7	22
$hH_2R + G_{s\alpha S}$	2.3 ± 0.4	6.3 ± 0.8	11.8 ± 0.5	42
$gpH_2R + G_{s\alpha S}$	1.5 ± 0.3	4.4 ± 0.5	10.8 ± 1.5	31
$rH_2R + G_{s\alpha S}$	4.9 ± 0.4	11.1 ± 1.3	16.1 ± 0.7	55
$cH_2R + G_{s\alpha S}$	12.8 ± 1.9	24.7 ± 4.1	31.1 ± 3.7	65
hH_2R-$G_{s\alpha S}$	12.1 ± 2.1	24.3 ± 4.8	28.7 ± 5.3	73
gpH_2R-$G_{s\alpha S}$	13.4 ± 3.1	25.0 ± 0.6	28.5 ± 2.2	77
rH_2R-$G_{s\alpha S}$	30.5 ± 2.6	43.5 ± 1.7	44.4 ± 3.0	94
cH_2R-$G_{s\alpha S}$	26.3 ± 3.6	41.9 ± 5.3	40.9 ± 5.2	107

$G_{s\alpha}$ fusion protein in combination with the determination of GTPase activity in Sf9 cell membranes was previously shown to be an appropriate system to quantify constitutive activity (Seifert et al., 1998b; Seifert and Wenzel-Seifert, 2002). This system fixes GPCR/G protein coupling and stays at a proximal level, thus avoiding potential bias caused by more downstream effects, such as effector activation or changes in gene expression. Moreover, due to the defined 1:1 stoichiometry of receptor and $G_{s\alpha}$ in fusion proteins, ligand potencies and efficacies in the steady-state GTPase assay are independent of the expression levels, allowing for the comparison of various membrane preparations with different expression levels (Seifert et al., 1999; Milligan, 2000).

We comprehensively characterized the human, guinea pig, rat, and canine H_2R species isoforms in steady-state GTPase assays in Sf9 cell membranes expressing H_2R-$G_{s\alpha S}$ fusion proteins. Structurally diverse H_2R full and partial agonists and antagonists unmasked considerable differences in the constitutive activities of the receptors. Specifically, cH_2R-$G_{s\alpha S}$ but neither rH_2R-$G_{s\alpha S}$ nor gpH_2R-$G_{s\alpha S}$ displayed the hallmarks of increased constitutive activity compared with hH_2R-$G_{s\alpha S}$ (Lefkowitz et al., 1993; Samama et al., 1993): 1) increased efficacies of partial agonists, 2) increased potencies of agonists with the extent of potency increase being correlated with the efficacy, and 3) increased inverse agonist efficacies and decreased potencies of antagonists.
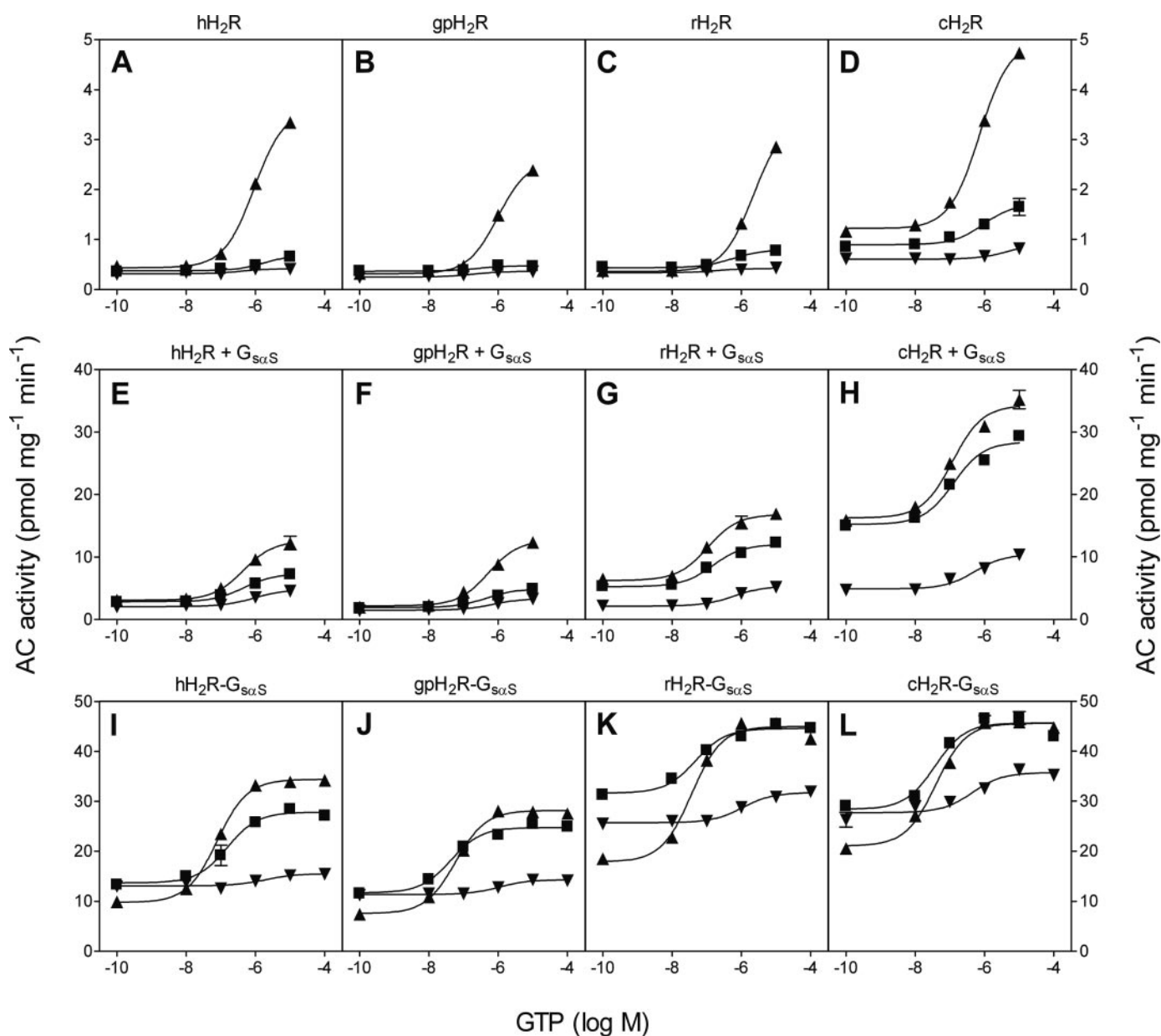
The determination of AC activity in Sf9 cell membranes is an alternative and sensitive method to investigate constitutive activity of GPCRs (Seifert et al., 1998a). With respect to AC, differences in the basal activity and in the magnitudes of signal increases upon stimulation with GTP are indicators for various levels of constitutive activity. In the AC activity assay with membranes expressing nonfused H_2R species isoforms either without or together with mammalian $G_{s\alpha S}$, both effects were most pronounced for canine relative to human, guinea pig, and rat, corroborating the outstanding role of cH_2R in terms of constitutive activity.

However, our analysis of AC activity in membranes expressing H_2R species isoforms also illustrates the limitations of this system. Most importantly, the low concentration levels of AC molecules constrain the maximal signal output, thereby yielding large stimulatory effects of GTP and large

inhibitory effects of inverse agonists on AC activity. In contrast, the stimulatory effects of the agonist HA are small, if at all detectable. In addition, in the case of the rH_2R, basal AC activities and the increases of AC activity upon stimulation with GTP were moderately higher compared with the hH_2R, whereas in the GTPase activity assay rH_2R-$G_{s\alpha S}$ and hH_2R-$G_{s\alpha S}$ showed similar constitutive activity. The accumulation of rH_2R in Sf9 cell membrane microdomains rich in AC molecules could be an explanation for the observed effects (Ostrom and Insel, 2004).

It is now widely accepted that GPCR activation involves disruption of an ionic lock between Asp(3.49) and Arg(3.50) of the highly conserved (E/D)RY motif in TM3 and Glu(6.30) in the cytoplasmatic extension of TM6 (Ballesteros et al., 2001; Visiers et al., 2002). The effects of mutations in the DRY motif on constitutive activity and structural instability of the rat H_2R were shown previously (Alewijnse et al., 2000). Asp-115(3.49), Arg-116(3.50), and Glu-228/229(6.30) are conserved among all H_2R species isoforms. However, preceding Glu-229(6.30) in hH_2R and gpH_2R and the corresponding Glu-228(6.30) in rH_2R, human, guinea pig, and rat H_2Rs exhibit an arginine (6.29), compared with a glycine (6.29), in cH_2R. Strikingly, many class A GPCRs contain a basic amino acid at the corresponding position, and accordingly, a stabilizing role of this residue in the network of ionic interactions was proposed (Ballesteros et al., 2001). Hence, the lack of this additional constraint in cH_2R could facilitate the transition from the inactive to the active state, resulting in the observed enhancement in constitutive activity.

Other differences in amino acid sequences could contribute to the differences in constitutive activity as well. Specifically, in G649, an allelic variant of the hH_2R, Asn-217 in i3, is replaced by Asp-217. This mutant displays low basal activity and is resistant to up-regulation upon antagonist exposure (Fukushima et al., 2001). Intriguingly, Asn-217 is conserved within hH_2R, gpH_2R, and rH_2R, but it is replaced by a histidine in cH_2R. Moreover, major variations in the sequences of H_2R species isoforms occur in the C-terminal domain. Because the C terminus of H_2R is important for G_s protein activation (Smit et al., 1996), the observed variations in the constitutive activities may alternatively or additionally be due to differences in this domain. In fact, an influence of the

Fig. 6. Regulation of AC activities in Sf9 membranes expressing H$_2$R species isoforms (A–D), H$_2$R species isoforms plus G$_{s\alpha S}$ (E–H), or H$_2$R-G$_{s\alpha S}$ fusion proteins (I–L). AC activity in Sf9 membranes was determined as described under *Materials and Methods*. Reaction mixtures contained Sf9 membranes expressing the proteins indicated on top of each panel and GTP at concentrations indicated at the abscissa. Reaction mixtures additionally contained H$_2$O (■), HA (100 μM) (▲), or IAPT (10 μM) (▼). Data shown are the means ± S.E.M. of one representative experiment performed in duplicates. The statistical analysis of AC activities is provided in Table 3. Data were analyzed by nonlinear regression and were best fitted to sigmoidal concentration-response curves. The control data for hH$_2$R-G$_{S\alpha S}$ and gpH$_2$R-G$_{S\alpha S}$ are identical with the control data for these constructs in Fig. 4 of Preuss et al. (2007).

C terminus on the constitutive activities of various GPCRs was described previously (Prezeau et al., 1996; Wenzel-Seifert and Seifert, 2003).

Ligand-Specific Interactions at H$_2$R Species Isoforms. In the GTPase activity assay, *N*-[3-(1*H*-imidazol-4-yl)propyl]guanidines and their *N*^{G}-acylated analogs were more potent and more efficacious at gpH$_2$R-G$_{s\alpha S}$ than at hH$_2$R-G$_{s\alpha S}$, which is in agreement with previous studies (Kelley et al., 2001; Xie et al., 2006a). Because both species isoforms exhibit similar constitutive activities, our present data further support the concept of distinct interactions as a rationale for this species selectivity. As was predicted by molecular modeling studies and subsequently verified by

site-directed mutagenesis, the species selectivity of guanidine-type agonists is based on two distinct amino acids, Tyr-17(1.31) in TM1 and Asp-271(7.36) in TM7 in the gpH$_2$R, presumably interacting via a charge assisted H-bond and thereby stabilizing an active agonist-bound conformation (Kelley et al., 2001). In the hH$_2$R [Cys-17(1.31), Ala-271(7.36)] and the rH$_2$R [Leu-17(1.31), Gly-270(7.36)], this interaction is impossible. Consistently, the guanidine-type agonists were similarly efficacious and potent at rH$_2$R-G$_{s\alpha S}$ and hH$_2$R-G$_{s\alpha S}$. Both cH$_2$R and hH$_2$R contain Cys-17(1.31) and Ala-271(7.36) and the differences in potencies and efficacies of the compounds between cH$_2$R-G$_{s\alpha S}$ and hH$_2$R-G$_{s\alpha S}$ were not specific to the guanidines. Thus, these

differences can be explained by the increased constitutive activity of cH_2R-$G_{s\alpha S}$ rather than by distinct ligand/GPCR interactions.

Recently, certain N^G-acylated guanidines have shown to be more efficacious than HA at gpH_2R-$G_{s\alpha S}$ in the GTPase assay (Xie et al., 2006b), similar to the observations made with UR-PG222A (**13**) in the present study. These effects can be attributed to the concept of ligand-specific gpH_2R conformations as well, i.e., these compounds stabilize active gpH_2R conformations that lead to more efficient interactions with $G_{s\alpha S}$ than achieved with the endogenous ligand HA. By analogy, at the β_2AR labeled with a fluorescent probe, the synthetic ligand isoproterenol induced a stronger change in fluorescence intensity than the endogenous ligand norepinephrine (Swaminath et al., 2004).

A further example of ligand-specific interactions at H_2R species isoforms is given by metiamide, acting as a weak partial agonist with low potency at cH_2R-$G_{s\alpha S}$ in the GTPase assay compared with being an inverse agonist with increased potency at human, guinea pig, and rat H_2R-$G_{s\alpha S}$. Moreover, in contrast to increased inverse agonist efficacies of antagonists **18** to **21** at cH_2R-$G_{s\alpha S}$ relative to hH_2R-$G_{s\alpha S}$, gpH_2R-$G_{s\alpha S}$, and rH_2R-$G_{s\alpha S}$, the inverse agonist efficacies of cimetidine (**17**), a cyanoguanidine analog of metiamide, were similar at all four species whereas its potency was significantly decreased at cH_2R-$G_{s\alpha S}$. Presumably because of the common 2[(5-methylimidazol-4-yl)methylthio]ethyl moiety, both metiamide and cimetidine stabilize distinct conformations in cH_2R relative to the other species isoforms, thus leading to an altered interaction with $G_{s\alpha S}$, which, in the extreme case of metiamide, causes weak partial agonism rather than increased inverse agonism.

Conclusions

In the present study, we demonstrate that the cH_2R exhibits increased constitutive activity compared with hH_2R, gpH_2R, and rH_2R. Species-specific differences in constitutive activity were previously reported for the cholecystokinin-B/gastrin receptor that, like the H_2R, stimulates gastric H^+ production (Kopin et al., 2000). Thus, differences in constitutive activities of GPCRs regulating H^+ production may reflect species-specific requirements for "basal" and peak H^+ secretion in the stomach. For example, following stimulation with HA, gastric acid secretion rates in dogs exceed those of the human (Kararli, 1995). Moreover, by studying the H_2R antagonist metiamide, further evidence for ligand-specific conformations of H_2R species isoforms was obtained. Our present study validates the notion that quantitative comparison of species isoforms of GPCRs provides unique insights into the molecular mechanisms of GPCR activation and ligand/GPCR interactions.

References

Alewijnse AE, Smit MJ, Hoffmann M, Verzijl D, Timmerman H, and Leurs R (1998) Constitutive activity and structural instability of the wild-type human H_2 receptor. *J Neurochem* **71**:799–807.

Alewijnse AE, Timmerman H, Jacobs EH, Smit MJ, Roovers E, Cotecchia S, and Leurs R (2000) The effect of mutations in the DRY motif on the constitutive activity and structural instability of the histamine H_2 receptor. *Mol Pharmacol* **57**:890–898.

Ballesteros JA, Jensen AD, Liapakis G, Rasmussen SG, Shi L, Gether U, and Javitch JA (2001) Activation of the β_2-adrenergic receptor involves disruption of an ionic lock between the cytoplasmic ends of transmembrane segments 3 and 6. *J Biol Chem* **276**:29171–29177.

Cheng Y and Prusoff WH (1973) Relationship between the inhibition constant (K_i) and the concentration of inhibitor which causes 50 per cent inhibition (I_{50}) of an enzymatic reaction. *Biochem Pharmacol* **22**:3099–3108.

Dove S, Elz S, Seifert R, and Buschauer A (2004) Structure-activity relationships of histamine H_2 receptor ligands. *Mini Rev Med Chem* **4**:941–954.

Elz S, Kramer K, Pertz HH, Detert H, ter Laak AM, Kühne R, and Schunack W (2000) Histaprodifens: synthesis, pharmacological in vitro evaluation, and molecular modeling of a new class of highly active and selective histamine H_1-receptor agonists. *J Med Chem* **43**:1071–1084.

Fukushima Y, Asano T, Saitoh T, Anai M, Funaki M, Ogihara T, Katagiri H, Matsuhashi N, Yazaki Y, and Sugano K (1997) Oligomer formation of histamine H_2 receptors expressed in Sf9 and COS7 cells. *FEBS Lett* **409**:283–286.

Fukushima Y, Oka Y, Saitoh T, Katagiri H, Asano T, Matsuhashi N, Takata K, van Breda E, Yazaki Y, and Sugano K (1995) Structural and functional analysis of the canine histamine H_2 receptor by site-directed mutagenesis: N-glycosylation is not vital for its action. *Biochem J* **310**:553–558.

Fukushima Y, Saitoh T, Anai M, Tsukuda K, Onishi Y, Sakoda H, Inukai K, Ogihara T, Funaki M, Ono H, et al. (2001) G649, an allelic variant of the human H_2 receptor with low basal activity, is resistant to upregulation upon antagonist exposure. *Pharmacogenomics J* **1**:78–83.

Gantz I, DelValle J, Wang LD, Tashiro T, Munzert G, Guo YJ, Konda Y, and Yamada T (1992) Molecular basis for the interaction of histamine with the histamine H_2 receptor. *J Biol Chem* **267**:20840–20843.

Gantz I, Munzert G, Tashiro T, Schäffer M, Wang L, DelValle J, and Yamada T (1991a) Molecular cloning of the human histamine H_2 receptor. *Biochem Biophys Res Commun* **178**:1386–1392.

Gantz I, Schäffer M, DelValle J, Logsdon C, Campbell V, Uhler M, and Yamada T (1991b) Molecular cloning of a gene encoding the histamine H_2 receptor. *Proc Natl Acad Sci USA* **88**:429–433.

Ghorai P (2005) *Arpromidine-Related Acylguanidines: Synthesis and Structure-Activity Relationships of a New Class of Guanidine-Type Histamine H_2 Receptor Agonists with Reduced Basicity*. Ph.D. thesis. University of Regensburg, Regensburg, Germany.

Gille A and Seifert R (2003) Co-expression of the β_2-adrenoceptor and dopamine D_1-receptor with $G_{s\alpha}$ proteins in Sf9 insect cells: limitations in comparison with fusion proteins. *Biochim Biophys Acta* **1613**:101–114.

Hill SJ, Ganellin CR, Timmerman H, Schwartz JC, Shankley NP, Young JM, Schunack W, Levi R, and Haas HL (1997) International Union of Pharmacology. XIII. Classification of histamine receptors. *Pharmacol Rev* **49**:253–278.

Houston C, Wenzel-Seifert K, Bürckstümmer T, and Seifert R (2002) The human histamine H_2-receptor couples more efficiently to Sf9 insect cell G_s-proteins than to insect cell G_q-proteins: limitations of Sf9 cells for the analysis of receptor/G_q-protein coupling. *J Neurochem* **80**:678–696.

Kararli TT (1995) Comparison of the gastrointestinal anatomy, physiology, and biochemistry of humans and commonly used laboratory animals. *Biopharm Drug Dispos* **16**:351–380.

Kelley MT, Bürckstümmer T, Wenzel-Seifert K, Dove S, Buschauer A, and Seifert R (2001) Distinct interaction of human and guinea pig histamine H_2-receptor with guanidine-type agonists. *Mol Pharmacol* **60**:1210–1225.

Kenakin T (2001) Inverse, protean, and ligand-selective agonism: matters of receptor conformation. *FASEB J* **15**:598–611.

Kopin AS, McBride EW, Schaffer K, and Beinborn M (2000) CCK receptor polymorphisms: an illustration of emerging themes in pharmacogenomics. *Trends Pharmacol Sci* **21**:346–353.

Lefkowitz RJ, Cotecchia S, Samama P, and Costa T (1993) Constitutive activity of receptors coupled to guanine nucleotide regulatory proteins. *Trends Pharmacol Sci* **14**:303–307.

Milligan G (2000) Insights into ligand pharmacology using receptor-G-protein fusion proteins. *Trends Pharmacol Sci* **21**:24–28.

Nederkoorn PH, van Gelder EM, Donne-Op den Kelder GM, and Timmerman H (1996) The agonistic binding site at the histamine H_2 receptor. II. Theoretical investigations of histamine binding to receptor models of the seven α-helical transmembrane domain. *J Comput Aided Mol Des* **10**:479–489.

Ostrom RS and Insel PA (2004) The evolving role of lipid rafts and caveolae in G protein-coupled receptor signaling: implications for molecular pharmacology. *Br J Pharmacol* **143**:235–245.

Preuss H, Ghorai P, Kraus H, Dove S, Buschauer A, and Seifert R (2007) Mutations of Cys-17 and Ala-271 in the human histamine H_2 receptor determines the species selectivity of guanidine-type agonists and increase constitutive activity. *J Pharmacol Exp Ther* **321**:975–982.

Prezeau L, Gomeza J, Ahern S, Mary S, Galvez T, Bockaert J, and Pin JP (1996) Changes in the carboxyl-terminal domain of metabotropic glutamate receptor 1 by alternative splicing generate receptors with differing agonist-independent activity. *Mol Pharmacol* **49**:422–429.

Ruat M, Traiffort E, Arrang JM, Leurs R, and Schwartz JC (1991) Cloning and tissue expression of a rat histamine H_2-receptor gene. *Biochem Biophys Res Commun* **179**:1470–1478.

Samama P, Cotecchia S, Costa T, and Lefkowitz RJ (1993) A mutation-induced activated state of the β_2-adrenergic receptor. Extending the ternary complex model. *J Biol Chem* **268**:4625–4636.

Seifert R, Lee TW, Lam VT, and Kobilka BK (1998a) Reconstitution of β_2-

adrenoceptor-GTP-binding-protein interaction in Sf9 cells: high coupling efficiency in a β_2-adrenoceptor-G$_s\alpha$ fusion protein. *Eur J Biochem* **255:**369–382.

Seifert R and Wenzel-Seifert K (2002) Constitutive activity of G-protein-coupled receptors: cause of disease and common property of wild-type receptors. *Naunyn-Schmiedeberg's Arch Pharmacol* **366:**381–416.

Seifert R, Wenzel-Seifert K, Bürckstümmer T, Pertz HH, Schunack W, Dove S, Buschauer A, and Elz S (2003) Multiple differences in agonist and antagonist pharmacology between human and guinea pig histamine H$_1$-receptor. *J Pharmacol Exp Ther* **305:**1104–1115.

Seifert R, Wenzel-Seifert K, and Kobilka BK (1999) GPCR-Gα fusion proteins: molecular analysis of receptor-G-protein coupling. *Trends Pharmacol Sci* **20:**383–389.

Seifert R, Wenzel-Seifert K, Lee TW, Gether U, Sanders-Bush E, and Kobilka BK (1998b) Different effects of G$_s\alpha$ splice variants on β_2-adrenoreceptor-mediated signaling. The β_2-adrenoreceptor coupled to the long splice variant of G$_s\alpha$ has properties of a constitutively active receptor. *J Biol Chem* **273:**5109–5116.

Smit MJ, Timmerman H, Blaauw J, Beukers MW, Roovers E, Jacobs EH, Hoffmann M, and Leurs R (1996) The C terminal tail of the histamine H$_2$ receptor contains positive and negative signals important for signal transduction and receptor down-regulation. *J Neurochem* **67:**1791–1800.

Swaminath G, Xiang Y, Lee TW, Steenhuis J, Parnot C, and Kobilka BK (2004) Sequential binding of agonists to the β_2 adrenoceptor. Kinetic evidence for intermediate conformational states. *J Biol Chem* **279:**686–691.

Traiffort E, Vizuete ML, Tardivel-Lacombe J, Souil E, Schwartz JC, and Ruat M (1995) The guinea pig histamine H$_2$ receptor: gene cloning, tissue expression and chromosomal localization of its human counterpart. *Biochem Biophys Res Commun* **211:**570–577.

Visiers I, Ebersole B, Dracheva S, Ballesteros JA, Sealfon S, and Weinstein H (2002) Structural motifs as functional microdomains in G-protein-coupled receptors: Energetic considerations in the mechanism of activation of the serotonin 5-HT$_{2A}$ receptor by disruption of the ionic lock of the arginine cage. *Int J Quantum Chem* **88:**65–75.

Wenzel-Seifert K, Liu HY, and Seifert R (2002) Similarities and differences in the coupling of human β_1- and β_2-adrenoceptors to G$_{s\alpha}$ splice variants. *Biochem Pharmacol* **64:**9–20.

Wenzel-Seifert K and Seifert R (2003) Functional differences between human formyl peptide receptor isoforms 26, 98, and G6. *Naunyn-Schmiedeberg's Arch Pharmacol* **367:**509–515.

Xie SX, Ghorai P, Ye QZ, Buschauer A, and Seifert R (2006a) Probing ligand-specific histamine H$_1$- and H$_2$-receptor conformations with N^G-acylated imidazolylpropylguanidines. *J Pharmacol Exp Ther* **317:**139–146.

Xie SX, Kraus A, Ghorai P, Ye QZ, Elz S, Buschauer A, and Seifert R (2006b) N^1-(3-Cyclohexylbutanoyl)-N^2-[3-(1H-imidazol-4-yl)propyl]guanidine (UR-AK57), a potent partial agonist for the human histamine H$_1$- and H$_2$-receptors. *J Pharmacol Exp Ther* **317:**1262–1268.

Address correspondence to: Dr. Roland Seifert, Department of Pharmacology and Toxicology, University of Regensburg, Universitätsstraße 31, D-93053 Regensburg, Germany. E-mail: roland.seifert@chemie.uni-regensburg.de